

Ionospheric Drift Motions and Velocities at UTHM's Parit Raja Station During Periods of Low Solar and Geomagnetic Activities

Abdull Zubi Bin Ahmad, Ahmad Faizal Bin Mohd Zain and Karthigesu Nagarajoo
Centre for Wireless and Radio Science (WARAS), UTHM

email: zubi3160@yahoo.com, dr_faizal@yahoo.com and karthi@uthm.edu.my

Abstract

Measurements relating to ionospheric plasma drift have been made by the Wireless and Radio Science Centre (WARAS) at Universiti Tun Hussein Onn Malaysia (UTHM) Parit Raja station in Batu Pahat, Johor, since 2004. This is done using a digital doppler interferometer which allows investigations into the dynamics of the ionosphere at this equatorial station to be carried out. These measurements include Doppler shifts and angles of arrival of the reflected HF signals that also allows simultaneous determination of plasma drift directions, drift distance covered and velocities as well as virtual heights of reflection, from ionospheric scattering point sources embedded within the moving plasma. By employing Doppler inteferometry reception technique at four receivers connected to four square array antennas nearby, it is possible to identify the locations, movements and velocities of the bulk scattering points reflected from the ionospheric F-region from the vertically incident HF waves. These waves are transmitted at frequencies of 6MHz, 7MHz, and 8MHz which cover the local F-layers since the critical frequencies lie between 5.9MHz and 8MHz. This work is based on data collected from the F2-layer of this local station at about 300km of virtual height during the measurement period of 2005.

Keywords: ionosphere, doppler interferometry, plasma drift, skymap

1. INTRODUCTION

Studies concerning the ionospheric plasma behaviour have been extensively carried out in the past. It is important to monitor the plasma drifts and convection since it brings new information related to the various phenomena that affect dynamic processes in the ionosphere.

In Malaysia, scientific interest in ionospheric research has intensified due largely to the need of modern military skywave and civilian navigation, satellite, together with over-the-horizon terrestrial communication systems. The research in these areas help provide propagation, navigation and positioning information as well as backup services for remote communications in times of disasters (eg., earthquakes and tsunamis).

Knowledge of the behaviour and variations of ionospheric plasma drifts with time, heights, solar cycles, geomagnetic storms as well as equatorial electrojets provide valuable data that are important for development of ionospheric forecast models [1].

To obtain a better understanding of ionospheric motions that affect signal propagations, advanced Doppler sounders using digital interferometric reception technique is being employed at the UTHM WARAS Centre for ground-based observations. This can provide detailed information regarding the structure and dynamics of the bottomside ionosphere at this station.

Apart from just acting as a vertical HF radar, this digital ionosonde is also able to measure more than just the roundtrip delay and amplitude of the reflected echoes; it also allows the determination of the plasma drift directions, and angle of arrival and Doppler frequency shifts of the received signal [2].

The technique relies on total reflection of the radio waves from the plasma structures that have plasma frequency f_N less than the vertically-incident radio frequency f . This way, the ionospheric F-region (probed up to about 1000km) is excited for up to a few hundred square kilometers.

Because of the non-uniform ionospheric surfaces and the volume inhomogeneities, the signal is reflected back from various reflection point sources to the Doppler interferometer at the ground for amplitude and phase processing

in the frequency domain where valuable data can be extracted for further analysis.

A study of plasma movements and its drift characteristics from measurements made is considered important in order to make comparisons with current modelling (theoretical or empirical) of the ionosphere or for development of future forecast models of ionospheric behaviour at this equatorial F-region station.

2. BASIC THEORY

The transmitted HF signal pulse at the digisonde's transmitting antenna can be represented by:

$$A(t) = u(t)\cos(2\pi f_o t) \quad (1)$$

where
amplitude

$A(t)$ = transmit HF signal

f_o = critical frequency of
transmission

$u(t)$ = Barker-coded waveform
that phase-modulate the
transmit carrier frequency

Due to the irregularities of the ionospheric layer, signals associated with each propagation mode may arrive at the receiver over a range of angles in both elevation and bearing. The received composite echo signal is given by:

$$r(t) = \sum_{s=0}^{N(t)} \alpha(t - \tau_s(t)) \cos[2\pi f_o(t - \tau_s(t)) + \varphi_{Ds}(t)] + n(t) \quad (2)$$

where

$N(t)$ = sum of s multipath
reflectors at

time of measurements

α = attenuation factor for the
echo

signal s delayed by τ_s

φ_{Ds} = time dependent Doppler
phase

shift

$n(t)$ = noise

With the received signal, a variation in the bearing or directions of arrival is also evident giving rise to positive and negative Doppler shifts. These are attributed to the reflections from the layers of ionospheric irregularities drifting across the points of reflections. From [3], the drift velocity is related by:

$$D_s = (1/\pi)v \cdot k_s \quad (3)$$

where s = index number of reflection point
 D = Doppler shift of reflection point at Rx
 v = reflecting plasma drift vector velocity
 k = unit vector from the ionospheric reflection point towards digisonde

3. MEASUREMENTS

The digisonde at WARAS is used to measure and monitor the plasma drift or convection behaviour as a function of time for the Parit Raja station located at latitude 1° 52' N and longitude 103° 48' E. The digisonde operates alternately between the ionogram mode and drift mode whereby the ionograms are spaced by fixed slots and the time in-between is filled with a number of F-region drift measurements from vertically-incident fixed HF frequencies of 5.9MHz.

The 4 receiving dipole antennas are arranged in a North-South and East-West configuration and co-located beside the delta-type transmitting antenna. The system also integrates a 13-bit (+1+1+1+1+1-1-1+1+1-1+1-1+1) Barker-coded phase coding technique that help minimise the need for much isolation between the transmitting and receiving antennas.

This 13-bit code binary-phase-modulate the transmitted RF frequency producing a digital BPSK compressed waveform with constant sidelobe levels at the output with radiation patterns that reduces interference between the transmitter and receiver antenna sidelobes. This will enhance the transmit power by 11dB or 13 times more at the output, giving an effective radiated power of about 7.8kW.

The technical specifications of the digisonde used in the measurements are given by the following table below:-

Table 1 Specification of Doppler Interferometer Used

1	Transmitter Peak Power	600W
2	Transmitter RF Frequency Range	1 – 20 MHz
3	Receiver Bandwidth	35 KHz
4	Pulse Repetition Frequency	40 Hz
5	Pulse Width	20 μsec
6	Range Resolution	3 Km
7	Pulse Compression	13-bit Barker code
8	Number of Receivers	4
9	Number of Receive Antennas	4
10	Dimension of Receive Dipole	25m

The receiver antenna array configuration are based on an arrangement proposed by Wright and Pitteway [4]. There are 4 dipoles along the centres of 4 sides of a 30m square. Each dipole is an untuned dipole of overall length 25m. The centre of each dipole is fed to a balanced high input impedance preamplifier. In order to make vector measurements related to plasma drift, the system is operated in a spaced receiver mode whereby the 4 antennas at the field are linked to the 4 identical phase-coherent receivers [5].

Drift measurements made with fixed transmitter frequencies of 5.9MHz, 7MHz, and 8MHz correspond to wavelengths (λ) over a range of 37.5m up to 50.8m. In terms of half-wavelengths ($\lambda/2$), these correspond to 18.75m up to 25.4m for half-wave dipole ($\lambda/2$) operation. Since the length of each receiver dipole used is 25m (see Table 1), it will cover up to the critical frequency of the F3-layer for this station (foF3 = 8MHz) [6].

For each sounding, the in-phase (I) and quadrature-phase (Q) amplitudes are measured for each of the 4 receivers. A drift measurement is made for 60 seconds interleaved between 5-minute intervals of ionogram measurements and consists of 20 μsec 6MHz HF soundings made at a pulse repetition frequency (PRF) of 40Hz. After A/D conversion, the 64-point FFT complex time series vectors for each duration bin for each antenna is then Fourier transformed in real-time. This way, the reflected echo amplitude and phase coefficients

of the composite signal can be estimated so as to be able to extract the basis functions representing the multipath echoes making up the received signal.

The generated skymap is then able to show the various reflection sources from the drift measurements which was carried out. This skymap displays the directional distribution as well as Doppler shifts of ionospheric echo sources in a horizontal view at this station. Further processing will also provide informations regarding the virtual heights of reflections as well as the drift distance covered by the plasma and the drift velocity attained.

4. RESULTS AND DISCUSSIONS

The earth's geomagnetic as well as solar indices are important ionospheric parameters that can have direct impacts on the local directional behaviour of plasma movements as well as the drift velocities attained. Magnetometer records obtained from the US National Oceanic and Atmospheric Administration (NOAA) for the year 2005 are used to reveal the variation of the earth's geomagnetic behaviour on the ionospheric plasma motion.

It can be seen that for almost 100% of the time, the monthly mean of the daily 3-hourly A average falls below 27. This value corresponds to a planetary geomagnetic index of $K_p \leq 4$ (ie. undisturbed geomagnetic activity) taken as an average over one month.

This indicates that the year 2005 can be regarded as an exceptionally quiet period with low geomagnetic activity. Figure 1 shows the variations of $K_p \leq 4$ for 2005 whereas Figure 2 displays the variations of the monthly mean of the daily A average for the same year.

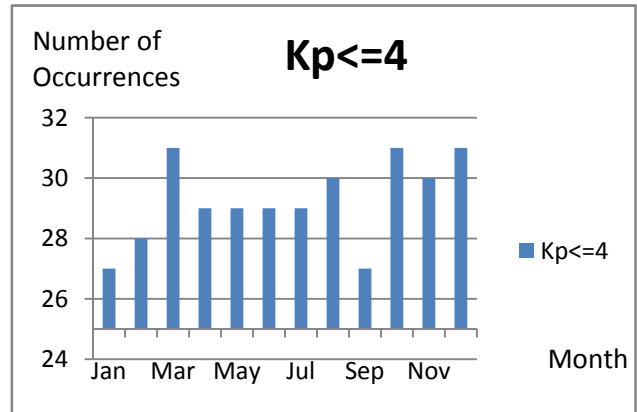


Fig 1 Barchart of Monthly $K_p \leq 4$ Variation for 2005

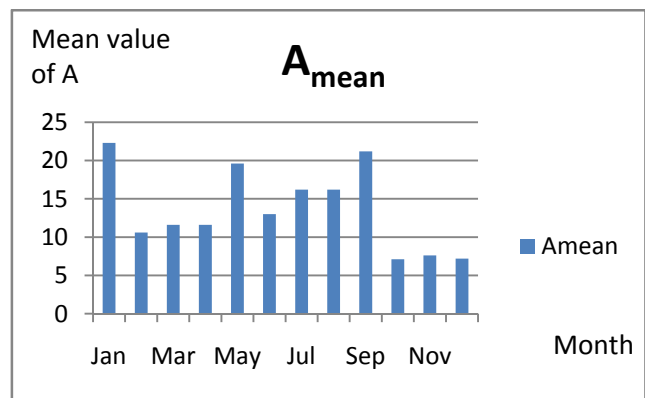


Fig 2 Barchart of Monthly A_{mean} Variation for 2005

Similarly, sunspot numbers (SSN) obtained from NOAA for the same year of 2005 are used to reveal the variation of the solar activities on the ionospheric plasma motion. This is summarised in Table 2(a) and Table 2(b) below.

Table 2(a) Variations of Solar SSN

Year	Jan	Feb	Mar	Apr	May	Jun
2000	90.1	112.9	138.5	125.5	121.6	124.9
2001	95.6	80.6	113.5	107.7	96.6	134
2002	114.1	107.4	98.4	120.7	120.8	88.3
2003	79.7	46	61.1	60	54.6	77.4
2004	37.3	45.8	49.1	39.3	41.5	43.2
2005	31.3	29.2	24.5	24.2	42.7	39.3
2006	15.3	4.9	10.6	30.2	22.3	13.9
2007	16.8	10.7	4.5	3.4	11.7	12.1
2008	3.3	2.1	9.3	2.9	3.2	3.4

Table 2(b) Variations of Solar SSN – contd.

Year	Jul	Aug	Sep	Oct	Nov	Dec
2000	170.1	130.5	109.7	99.4	106.8	104.4
2001	81.8	106.4	150.7	125.5	106.5	132.2
2002	99.6	116.4	109.6	97.5	95.5	80.8
2003	83.3	72.7	48.7	65.5	67.3	46.5
2004	51.1	40.9	27.7	48	43.5	17.9
2005	40.1	36.4	21.9	8.7	18	41.1
2006	12.2	12.9	14.4	10.5	21.4	13.6
2007	9.7	6	2.4	0.9	1.7	10.1
2008	0.8	0.5	1.1	2.9	4.1	0.8

Plots of SSN variations are given in Figure 3(a) and 3(b). Comparing with the yearly SSN variations from 2000-2008, it can be seen that 2005 can also be considered as a year with an exceptionally quiet solar activity with an average recording of 29.7 for the SSN taken over one year.

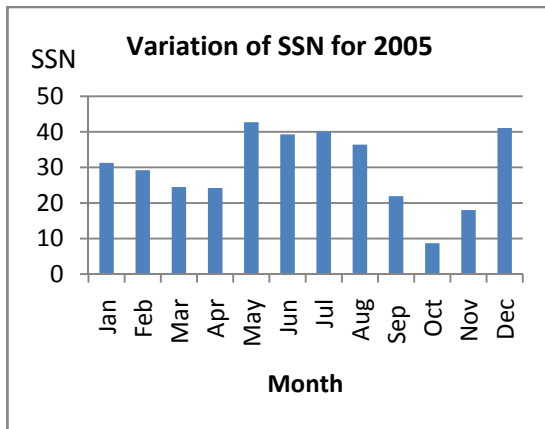


Fig 3(a) Bargraph of Monthly SSN for 2005

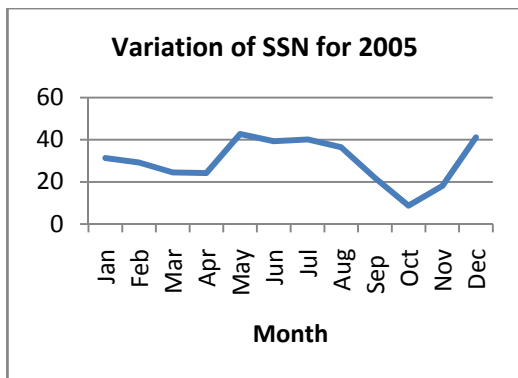


Fig 3(b) Linegraph of Monthly SSN for 2005

From the measurements made, processing of the reflected echoes begins by forming the cross spectra from the saved spectrum segments for each of the E-W and N-S antenna pairs. Each saved FFT bin has significant power and is assumed to correspond to an ionospheric reflection point or source.

The skymap display shows the reflection points drift direction as well as Doppler shift. The observable trend across the skymap indicates the bulk horizontal motion of the ionospheric reflection sources.

Several assumptions are made in this study. It is assumed that there is minimal refraction effects since only the bottomside of the ionosphere is probed and that the plasma is moving with a uniform bulk flow. This also means that the reflection point sources being detected by the doppler interferometer are actually embedded in the bulk flow. This assumption is reasonable as only the cluster of reflection points with a pronounced ‘cloud’ having a dominant horizontal convection pattern in either the North-South (N-S) or East-West (E-W) directions are considered. In addition to that, for plasma motion determination above the doppler interferometer, the most relevant echo points for consideration should have incidence angles towards the receiving antennas that are close to vertical. Therefore point sources with a maximum zenith angle of 45° have been selected.

The following results obtained shows the movement of plasma in various directions representing north, south, east, west, northwest, northeast, southwest, southeast and central locations as shown in Table 4(a) and 4(b). The percentage of drift by directions is also shown in Figure 4.

Table 4(a) Drift Directions for 2005

Month	N	%	S	%	E	%	W	%	NW	%
Jan	2	8	2	8	13	50	2	8		0
Feb	1	4	4	16	7	28	6	24	1	4
Mar	1	5	3	15	4	20	2	10		0
Apr		0	1	11	3	33	1	11	2	22
Aug									31	100
Sep									30	100
Oct							18	60	12	40
Nov							30	100		
Dec							19	61	12	39
Tot%	2		4		11		33		38	

Table 4(b) Drift Directions for 2005 – contd

Month	NE	%	SW	%	SE	%	C	%
Jan	1	4		0	2	8	4	16
Feb	2	8	1	4	4	16	2	8
Mar	1	5	4	20	2	10	3	15
Apr	1	11		0	1	11		0
Aug								
Sep								
Oct								
Nov								
Dec								
Tot%	2		2		4		4	

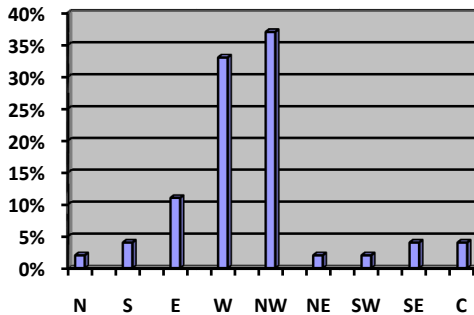


Fig 4 Percentage of Drift by Directions for 2005

A typical skymap display is shown in Figure 5 and a summary of plasma drift trend is also given in Table 5 which shows the behaviour of plasma motion for each month of the year for which data have been collected and analyzed. There are no data available for the months of May to July for that particular year.

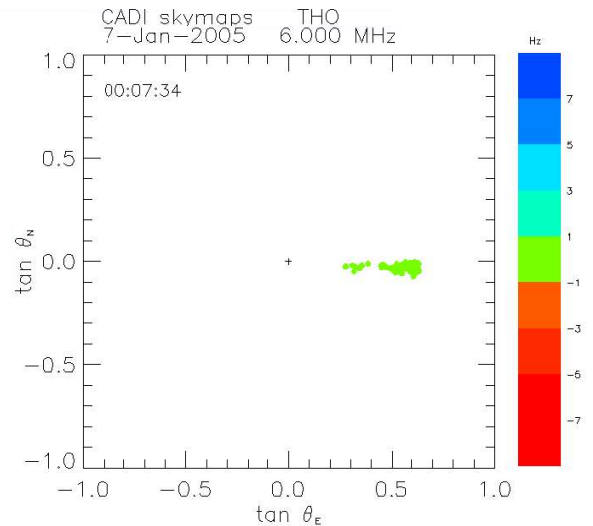


Fig 5 Typical Easterly Skymap Display for 2005 with +/-1Hz Doppler shift

Table 5 Summary of Plasma Drift Trend for 2005

Month	Drift Trend/Behaviour
January	drift dominant in easterly direction
February	irregular drifts, no clear directions
March	irregular drifts, no clear directions
April	irregular drifts, no clear directions
May	Data not available
June	Data not available
July	Data not available
August	drift purely in northwesterly direction only
September	drift continues purely in north-westerly direction for second successive month
October	drift starts to shift westward from north-westerly direction
November	drift fully westward for this month
December	drift shifts from purely westward in previous month to north-westerly this month
Whole Year (2005)	drift for the whole year is dominated by westerly and north-westerly directions

In addition, the following results represent the maximum local plasma drift velocity magnitudes that have been analyzed and compiled for the month of January 2005 for Parit Raja station:-

Table 6(a) Drift Velocity Magnitudes for Jan 2005

Day	East-West	LT	North-South	LT
1	25m/s	1130	40m/s	2130
2	40	2030	40	2230
3	5	1430	10	1430
4	40	2130	50	2000
5	50	0430	20	0430
6	50	2100	20	2030
7	50	2300	50	2230
8	10	2400	30	2230
9	25	1830	35	2000
10	50	2000	40	2100
11	90	2330	50	2330
12	10	1230	30	1900
13	100	2330	100	2350
14	120	2300	30	2300
15	120	2200	30	2300

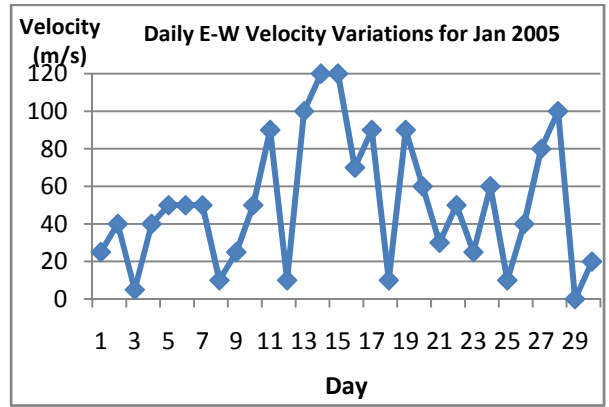


Fig 6 Daily East-West Plasma Motion Velocity Variations

Table 6(b) Drift Velocity Magnitudes for Jan 2005- contd.

Day	East-West	LT	North-South	LT
16	70	2300	100	2200
17	90	0200	90	0600
18	10	1800	35	2030
19	90	2130	80	2130
20	60	2330	40	2200
21	30	0900	30	1000
22	50	2030	40	2100
23	25	2030	10	0830
24	60	2130	90	2200
25	10	2030	50	2130
26	40	2130	80	2030
27	80	2130	50	2130
28	100	2030	10	1930
29	N/A	N/A	10	2130
30	20	2300	70	0900

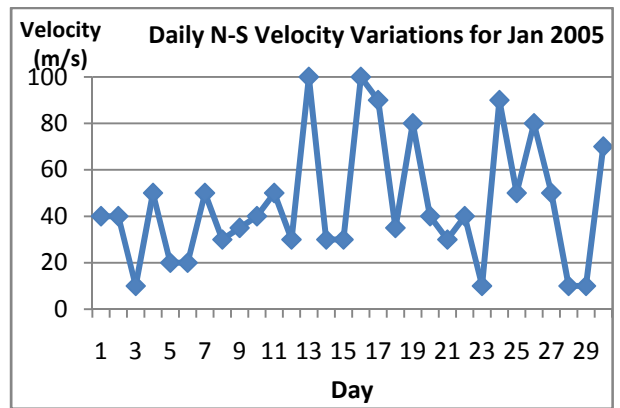


Fig 7 Daily North-South Plasma Motion Velocity Variations

From the above table, the following plots can be made:-

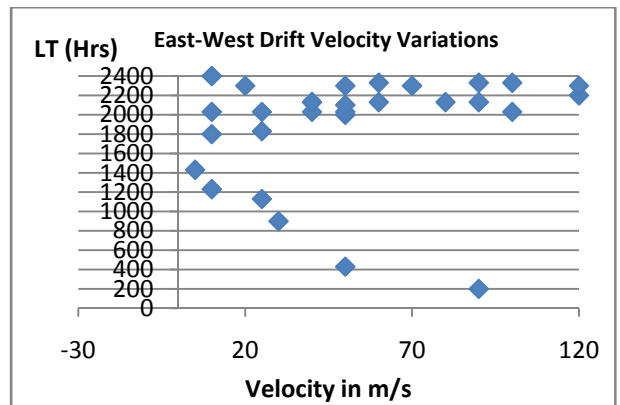


Fig 8 Probable Time Occurrence of E-W Velocity Spread

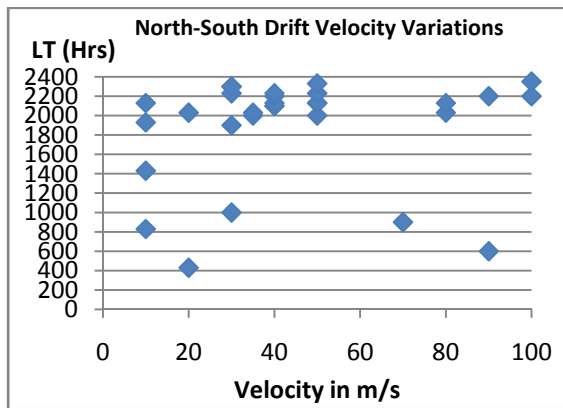


Fig 9 Probable Time Occurrence of N-S Velocity Spread

5. CONCLUSIONS

Since 2005 is exceptionally quiet, with low geomagnetic as well as solar activity, it can be postulated that the plasma motion recorded in this study is due to the presence of local causes like strong effects due to regional prevailing ionospheric winds in this equatorial zone. The wind contribution would have more prominent influence than the effects of the earth's geomagnetic activity or the sun's solar behaviour, which are minimal.

In so far as the plasma drift velocity is concerned, the East-West direction registers a maximum speed of 120m/s whereas the North-South direction reaches a maximum speed of 100m/s. It can also be observed from the plots that the plasma drift velocity magnitudes occur randomly due to the prevailing ionospheric winds and do not have a correlation with any day of the month. The last two figures indicate that these moving plasma changes velocities for the most part during local times from 1800 Hrs to 2400 Hrs.

6. ACKNOWLEDGEMENT

The author would like to thank Universiti Tun Hussein Onn Malaysia (UTHM) for providing the funding for the Wireless and Radio Science (WARAS) Centre. Waras operates the first and only digital ionosonde in Malaysia.

REFERENCES

- [1] Mikhailov, A., *Short-term foF2 Forecast: Present day State of the Art*, Second European Space Weather Week, 2005
- [2] Reinisch, B.W., *Modern Ionosondes*, Modern Ionospheric Science, European Geophysical Society, 1996
- [3] Cannon, P.S., B.W. Reinisch, J. Buchau, and T.W. Bullett, *Response of Polar Cap F-Region Convection Direction to Changes in the IMF: Digisonde Measurement in Northern Greenland*, *J Geophysics Res*, 96 (AZ) 1239-1250
- [4] Wright, J.W. and M.L.V. Pitteway, *Realtime Acquisition and Interpretation Capabilities of the Dynasonde2 : Determination of Magnetoionic Mode and Echolocation Using Spaced Receiving Arrays*, *Radio Science*, 14, 828-835 (1979)
- [5] J.W. MacDougall, I.F. Grant, and X Shen, *The Canadian Advanced Digital Ionosonde : Design and Results*
- [6] Mohd Kamal Jaafar, A.F.M. Zain, *Short-term Statistical Analysis of the Occurrence of the F3 Layer in Malaysian Ionosphere for Winter 2004*
- [7] Bittencourt, J.A. and Abdu, M.A., *J Geophysics Res* 86, 2451-2454
- [8] Jayachandran, B, S.P. Namboothiri, N Balan, P.B. and J.H. Sastri, *HF Doppler Radar Observations of Equatorial Plasma Drifts and Spread-F*
- [9] National Oceanic and Atmospheric Administration, http://www.ngdc.noaa.gov/stp/geomag/kp_ap.htm

APPENDIX - (Analyzed geomagnetic data for 2005)

[NB]: Percentage of $K_p \leq 4$ is about 95% for 2005

Kp	0	1	2	3	4	5	6	7	8	9	Mean of Daily A Average	Number of days Kp≤4 in a month
JAN	14	45	45	62	40	15	13	6	2	0	22.3	27
FEB	17	68	61	47	25	5	1	0	0	0	10.6	28
MAR	19	74	61	54	24	12	1	0	0	0	11.6	31
APR	12	67	87	36	25	8	1	2	0	0	11.6	29
MAY	5	49	63	66	35	10	9	2	1	1	19.6	29
JUN	6	58	92	45	23	10	3	1	0	0	13.0	29
JUL	0	46	78	62	31	17	6	0	0	0	16.2	29
AUG	5	38	88	63	25	12	3	1	1	1	16.2	30
SEP	6	38	72	48	33	21	12	3	0	1	21.2	27
OCT	53	85	55	36	16	0	0	0	0	0	7.1	31
NOV	44	69	68	38	14	1	0	0	0	0	7.6	30
DEC	61	74	51	38	11	4	0	0	0	0	7.2	31
TOTAL	242	711	821	595	302	115	49	15	4	3	164.2	351 (95%)
Kp %	8.5	24.9	28.7	20.8	10.6	4.0	1.7	0.5	0.1	0.1		(out of 365)

